Performance Analysis of the Chena Binary Geothermal Power Plant

Mathew Aneke, Brian Agnew, Chris Underwood

Accepted Manuscript

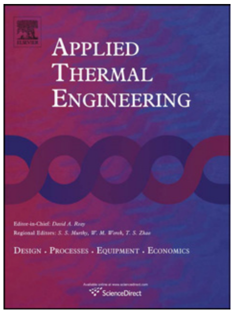

Title: Performance Analysis of the Chena Binary Geothermal Power Plant

Authors: Mathew Aneke, Brian Agnew, Chris Underwood

PII: S1359-4311(11)00109-8

DOI: 10.1016/j.applthermaleng.2011.02.028

Reference: ATE 3439

To appear in: *Applied Thermal Engineering*

Received Date: 18 October 2010

Revised Date: 21 January 2011

Accepted Date: 16 February 2011

Please cite this article as: M. Aneke, B. Agnew, C. Underwood. Performance Analysis of the Chena Binary Geothermal Power Plant, Applied Thermal Engineering (2011), doi: 10.1016/j.applthermaleng.2011.02.028

Performance Analysis of the Chena Binary Geothermal Power Plant

***Mathew Aneke, Brian Agnew, Chris Underwood**
School of Built and Natural Environment, Northumbria University, Newcastle upon Tyne, United Kingdom, NE1 8ST

Abstract

In this paper, the IPSEpro Model of the Chena Geothermal ORC power plant had been developed and validated using the real data. The validated model was used to investigate the effect of variation in the geothermal source temperature on plant performance.

The analysis showed that the variation of the geothermal source temperature affects the plant behaviour. Increase in the geothermal source temperature above the design point increases the working fluid flowrate, decreases the working fluid degree of superheat at the inlet of the turbine (evaporator exit), increases the plant net power output and reduces the efficiency while decrease in the geothermal source temperature lower than the design point increases the degree of superheat up to a certain maximum beyond which it starts to reduce. It also causes a decrease in the net power output and an increase in the plant efficiency.

Keywords: Organic Rankine Cycle (ORC), IPSEpro, Geothermal, Power Generation

***Correspondence Author**: mathew.aneke@unn.ac.uk; +447501893347

Nomenclature

		Subscripts	
ε	Heat Exchanger Effectiveness	1,2,3,...,7	State Points
$\eta_{thermal}$	Thermal efficiency	*cin*	Cold Fluid Inlet
$\varkappa$	Working Fluid Enthalpy Parameter	*G*	Generator
C	Heat Capacity Rate (kW/K)	*hin*	Hot Fluid Inlet
NTU	Number of Transfer Units	*max*	Maximum
Q	Heat transfer Rate (kW)	*min*	Minimum
T	Temperature (^{o}C or K)	*o*	Saturated Liquid
UA	Thermal Conductance (kW/K)	*P*	Pump
W	Power (kW)	*s*	Saturated Vapour

1 Introduction

The world population and industrialisation had been on the increase. This had resulted in a tremendous increase in the global energy demand. Over 80% of the global energy supply comes from the fossil fuels [1]. Hence since fossil fuels are exhaustible, there is need for its conservation.

Despite that, the over dependence on fossil fuels for energy supply had resulted in the release of large quantity of anthropogenic CO_2 (greenhouse gas) into the environment; causing environmental pollution and global warming. This associated environmental danger caused by the burning of fossil fuels had resulted in a clamour by the world leaders to develop better and more efficient means of meeting the world energy demand at the least possible environmental impact.

Recently, there has been a gradual shift from the over dependence on fossil fuels to the use of renewable and cleaner energy sources like wind energy, solar energy, geothermal energy and so on.

Geothermal heat energy is a renewable heat energy which comes from beneath the earth surface with temperatures varying from 50 to 350 ^{o}C [2]. It occurs mainly in the form of steam, mixtures of steam and water or just liquid water.

Geothermal heat energy had been identified as a good source of power for over ten decades. The first demonstration on power generation from geothermal source occurred in 1904 at Larderello, Italy [3]. The success of this demonstration resulted in the rapid increase in the use of geothermal energy and by 1942, the installed geothermal-electric capacity in Italy rose to about 127650 kW_e [3]. From there, the utilisation of geothermal energy for electricity generation spread to other parts of the world with countries like Japan, USA, New Zealand, and Mexico exploiting their first geothermal energy in 1919, 1921, 1958, and 1959 respectively [3]. By 2003, the estimated installed geothermal capacities had risen to about 8402.21 MW_e.

The first set of geothermal power plants makes use of conventional steam turbines which require fluids at temperatures of at least 150 ^{o}C. This resulted in the non-utilization of the low and medium temperature geothermal for power generation. However, with the development of binary cycle power plants (Organic Rankine Cycle (ORC) and Kalina Cycle) technology, the low and medium temperature geothermal in the temperature range 70 – 100 ^{o}C and 100 – 150 ^{o}C respectively are now utilised for power generation. The only major difference between the conventional steam turbine and the binary system is that in the former the steam or hot water from the geothermal reservoir passes directly through the turbine while in the later, the steam or hot water is used to vapourise an organic working fluid which is expanded in the turbine.

The idea of utilising organic working fluid was borne as far back as 1823 [4]. Ever since then, researches had been going on to determine the effect of working fluid on the performance of ORC systems [5] as well as to determine the best working fluid for ORC applications [2], however, most results had shown that different working fluids show different performance at different operating conditions. Hence the working fluid chosen for any application is a function of the operating condition, cost, safety and the environmental impact.

ORC systems have made their appearance in the market of power generation systems as a valid substitute for the conventional steam cycles [6]. Although the cost of conventional steam turbine power plants seems to be lower than that of the binary power plants [2], the ability of the later to utilise low temperature geothermal energy, industrial waste heat energy, solar energy for electricity generation as well as its high flexibility and reliability with low maintenance and supervision makes it very attractive.

This paper is focused on simulation and validation of an existing ORC geothermal power generation plant located in Chena, Alaska, USA, using the IPSEpro Process Simulation Software. A parametric study of the power plant behaviour as the geothermal source temperature varies is also evaluated using the validated power plant model.

Chena is a city in Alaska, USA. It has a hot spring located approximately 96560 m east-northeast of Fairbanks, at an elevation of 367 m [7]. The hot spring has been used to a great extent for recreational activities since its discovery in 1905.

Holdmann [7] in the 2007 paper prepared for Alaska Energy Authority reported that the cost of electricity in rural Alaska is among the highest in USA with most of the electricity supply from generator sets. He reported that in 2005, $365,000 was spent on fuel alone for power generation at Chena. This high cost of power generation motivated Chena to seek for alternative power supply system which thus, resulted in the adoption of the plan to increase the energy independence using geothermal resources available in the area.

Of all the processes of power generation from low temperature geothermal heat source evaluated, the ORC system provided by United Technologies (UTC) was selected as the most promising because of the inherent low cost achieved through the use of inexpensive, mass produced, U.S. manufactured air conditioning and refrigeration equipments from Carrier Refrigeration [7, 8]. The successful implementation of this project had resulted in the reduction in electricity cost at Chena from 30 cents per kWh to 5 cents per kWh [7].

2 Process Diagram of ORC

Figure 1 shows the process flow diagram of the ORC system using geothermal heat source. In the process, the geothermal hot water/steam from the reservoir is used to preheat and vapourise the organic working fluid in the evaporator. The vapour from the evaporator passes through the turbine where it expands to produce work which is used to turn the shaft connected to the generator to generate electricity. The low pressure organic working fluid vapour from the turbine is then passed through the condenser where it is condensed to liquid using cold water. The liquid organic working fluid is then pumped back to the evaporator to complete the cycle and the whole process restarts again.

Figure 1: Process Flow Diagram of ORC System Utilising Geothermal Heat Source

3 IPSEpro Simulation of the Chena Geothermal Power Plant

The IPSEpro model of the Chena power plant was developed using IPSEpro Simulation Software Version 4.0 [9]. IPSEpro is modular-mode as well as equation-oriented steady state energy simulation software. It contains Model Development Kit (MDK) and Process Simulation Environment (PSE) packages. The (MDK) contains the libraries in IPSEpro. The libraries are made up of modules of unit operations (like heat exchangers, turbine, combustion units and so on) in which are embedded the model design equations, connections (like process streams, utility streams and so on) in which are embedded the physical property calculators, and the global library (ambient, fuel composition etc). The model equations used to model the individual unit operations and the physical properties calculator used to model the process streams in IPSEpro were standard equations obtainable from the literature [9]. The PSE makes use of the model libraries in MDK to develop and simulate the model of any given system.

In order to develop the IPSEpro PSE Model of the Chena Geothermal Power Plant presented in this paper, the relevant unit operation modules (evaporator, turbine, condenser, generator, pump and motor) and process streams (R134a, hot geothermal source and cooling water) from the MDK library were used.

The temperatures and mass flow rates of the geothermal and cooling water source were the same as that used in the real power plant at Chena (see Table 1) [7].

Table 1: Geothermal and Cooling Water Source Temperature and Mass Flowrate

The organic working fluid (R134a) used in the power plant model was the same as that used in the real plant at Chena [7]. The thermodynamic properties of the working fluid shown in Table 2 are obtained from REFPROP version 7.0 [10].

Table 2: Thermodynamic Properties of R134a (CF_3CH_2F – 1,1,1,2 – tetraflouroethane (CAS# 811-97-2))

The simulated IPSEpro PSE Model of the Chena ORC power plant at the nominal operating condition (design point) is shown in Figure 2.

Figure 2: IPSEpro PSE Model of the Chena Geothermal Power Plant at the Design Operating Condition

The power plant thermal efficiency $\eta_{thermal}$, heat exchangers (condenser and evaporator) NTU value, and effectiveness ε, were determined using the standard equations presented below:

The thermal efficiency of the plant, $\eta_{thermal}$ was calculated using the equation 1

$$\eta_{thermal} = {(\mathrm{W}_G - \mathrm{W}_P)}/{\mathrm{Q}_{input}} \quad (1)$$

where,

$\mathrm{W_G}$ = Total power produced in the generator

$\mathrm{W_P}$ = Total power consumed by the pump

Q_{input} = Total energy input from the geothermal heat source to the preheater /evaporator

The Number of Transfer Unit (NTU) of the heat exchangers was calculated using equation 2

$$NTU = {UA}/{C_{min}} \quad (2)$$

where

C_{min} = Smaller heat capacity rate of the fluids that passes through the heat exchanger

In a heat exchanger which involves a phase-change of one of the fluids, the effective specific heat for the phase-changing fluid is infinity, therefore $\mathrm{C_{min}}$ is the heat capacity of the non-phase changing fluid (water in this case) for both the evaporator and the condenser [11].

The effectiveness (ϵ) of the heat exchangers was calculated using equation 3 shown below:

$$\varepsilon = {\mathrm{Q}}/{\mathrm{Q}_{max}} \quad (3)$$

where

Q = Actual heat transfer rate in the heat exchanger

Q_{max} = Maximum heat transfer rate in the heat exchanger

$$\mathrm{Q}_{max} = \mathrm{C}_{min}(\mathrm{T}_{hin} - \mathrm{T}_{cin}) \quad (4)$$

where

T_{hin} = Inlet temperature of the hot fluid to the heat exchanger

T_{cin} = Inlet temperature of the cold fluid to the heat exchanger

The state of the working fluid, at the exit/inlet of any given unit operation is defined using the enthalpy parameter, $\varkappa$ which is calculated as

$$\varkappa = {(h - h_o)}\big/{(h_s - h_o)} \qquad (5)$$

where,

$h =$ Specific enthalpy of the stream at any given pressure

h_o= Specific saturated liquid enthalpy of the stream at the same pressure

$h_s =$ Specific saturated vapour enthalpy of the stream at the same pressure

From the definition of $\varkappa$, it can be seen that $\varkappa < 0$ when the stream is at the sub-cooled phase, $\varkappa = 0$ when the stream is saturated liquid, $0 < \varkappa < 1$ when the stream is at the two-phase region, $\varkappa = 1$ when the stream is saturated vapour, and $\varkappa > 1$ when the stream is at superheated phase.

The values of $W_G, W_P, UA, Q, Q_{input}, h_o, h_s, and\ h$ were obtained from the IPSEpro Simulation result.

4 Results & Discussion

Model Validation

The developed model is simulated using the IPSEpro PSE package. The thermodynamic processes and the thermodynamic cycle exhibited by the working fluid are shown in Table 3 and Figure 3 respectively. The heat exchangers (evaporator and condenser) T-Q diagram showing the heat exchangers pinch temperatures at the design point are shown in Figures 4 and 5 respectively.

Table 3: Thermodynamic Processes Exhibited by the Working Fluid (R134a)

Figure 3: Thermodynamic Cycle of the Working Fluid (R134a)

Figure 4: Evaporator T-Q diagram

Figure 5: Condenser T-Q diagram

The simulation result was validated with the real plant design data from the Chena Geothermal Power plant. The validation was done by comparing the simulation result with the real plant design data at the nominal design point as shown in Table 4. From the table, it can be seen that the real plant data matches the simulated result very well. Hence this model can be used to carry out performance analysis case study of the real plant.

Table 4: Validation of Plant IPSEpro Model with the real Chena Geothermal Power Plant Design Data

Performance Analysis of the Chena Geothermal ORC Power Plant using the Validated IPSEpro PSE Model

The case study carried out in this paper is neither an optimisation case study nor a design case study. The case study intends to investigate the behaviour of an already designed, fabricated and commissioned ORC power plant when there are changes in the nominal design conditions. Hence, it is different from most of the case studies found in the literature which are mainly focused on optimising the performance of the ORC power plant at the nominal design condition.

In order to carry out this case study so that it will represent a real plant system, some plant parameters were fixed at values similar to that of the validated design point while some are allowed to vary. The fixed variables are set based on the following assumptions:

- For a power plant such as Chena Geothermal ORC Power Plant which had been designed to operate at maximum performance at the nominal design conditions, the overall UA values of the heat exchangers (evaporators and condensers) [12] and the pressure drops in the units of equipment are likely to be constant. Based on this argument, the UA values of the heat exchangers and the pressure drop in the unit of equipments were fixed at the same value as the validated model.

- The temperature of the working fluid at the entrance to the evaporator is fixed to the value similar to that used for the model validation.

- Furthermore, Chena Geothermal Power Plant like most other geothermal power plants makes use of re-injection of the used geothermal fluid into the re-injection wells in order to improve the pressure on the production wells. One problem usually associated with re-injection operation is the cooling of the geothermal fluid by the used fluid which is re-injected into the production well. In order to avoid this problem, most of the re-injection wells are designed to determine the best location for the re-injection well and the best temperature at which used geothermal fluid will be re-injected to achieve the desired pressure and avoid the cooling of the geothermal fluid. Based on this argument, the exit temperature of the geothermal fluid is fixed at the same value as the validated model.

- The cooling water used in the Chena ORC power plant is discharged in a Monument Creek via an existing drainage ditch. This discharge is regulated by the Department of Natural Resources (DNR) and Chena has a permit for discharging the cooling water effluent [7]. Since the cooling water discharge is regulated, there is a tendency that the cooling water discharge temperature should be maintained at a certain level to avoid an unwanted environmental impact. Based on this argument, the exit temperature of the cooling water from the geothermal power plant is set at the same value as the validated model.

- The working fluid pump is assumed to be a variable speed pump. This is used to maintain the pressure at the inlet of the turbine which is fixed at the same value as the as the validated model.

Based on the above arguments, the performance case study of the Chena Geothermal ORC power plants was carried out by fixing some variables of the validated Chena Geothermal ORC Power Plant model as shown in Table 5**Error! Reference source not found.**.

Table 5: Fixed Variables of the Chena Power Plant Model for Performance Case Study

Effect of Variation in Geothermal Source Temperature on Plant Behaviour

Using the nominal design point as the reference point, the effect of variation in the geothermal source temperature from 61 ^{o}C to 80 ^{o}C were investigated using the validated IPSEpro Model of the Chena Geothermal ORC Power Plant.

Figure 6 shows the changes in plant power output and thermal efficiency when the geothermal source temperature changes from 61 ^{o}C to 80 ^{o}C. Using the plant design geothermal source temperature of 73.33 ^{o}C as the reference point, it can be seen from the graph that when the source temperature goes lower than the design point, the plant thermal efficiency first increases to a maximum of 8.8 % at 65 ^{o}C after which it starts to decrease while the net power output continues to decrease. On the other hand, if the geothermal source temperature increases higher than the design point, the thermal efficiency decreases while net power output increases up to a maximum of 216 kW at a source temperature of 76 ^{o}C beyond which any further increment in the source temperature lowers the plant net power output. This behaviour occurs because when the geothermal source temperature increases higher than the design temperature, the system characteristics demands that more working fluid will be vapourised in the evaporator. In order to meet up with the system demand, the working fluid flowrate increases (see Figure 8) and so does the power required by the pump (see Figure 7). The increase in the working fluid flow rate initially produces more power than the additional power consumed by the pump and hence the net effect causes an initial increase in the plant net power output up to a maximum value (as shown in Figure 6) beyond which the effect of the power consumption by the pump overtakes the additional gross power generation caused by increase in working fluid flow rate hence producing a lower net power output. The increase in source temperature also causes an increase in the heat input to the system thus causing a decrease in the thermal efficiency of the plant. Furthermore, a decrease in the geothermal source temperature lower than the design temperature causes a decrease in the quantity of working fluid vapourised in the evaporator and this leads to a decrease in the net power output. This also causes a decrease in the heat input to the system thus producing an increase in thermal efficiency up till the point where it peaks after which it continuously falls again. This behaviour in the plant thermal efficiency is similar to that obtained in the one year experience report prepared by the Chena Geothermal ORC plant personnel [8].

Figure 6: Effect of Variation in Geothermal Source Temperature on Plant Efficiency & Net Power Output

Figure 7: Effect of Variation in Geothermal Source Temperature on Pump Power Consumption

Figure 8 shows the variation in the working fluid enthalpy parameter, $\varkappa$ at the turbine inlet (evaporator exit) and the working fluid flowrate as the geothermal source temperature changes. Using the plant design point as the reference, increasing the geothermal source temperature decreases the working fluid enthalpy parameter, $\varkappa$ (thus lowering the degree of superheat) at the turbine inlet while lowering the geothermal source temperature increases the working fluid enthalpy parameter, $\varkappa$ up to a peak value of 1.04 at geothermal source temperature of 70 ^{o}C after which it starts to decrease gradually. This behaviour occurs because when the geothermal source temperature increases beyond the design point, more working fluid flows through the system (see Figure 8) and thus through the evaporator. Since the evaporator has a fixed heat exchanger area and is designed for a lower working fluid flowrate; the heat exchanger area will not be enough to superheat the working fluid and thus this causes a decrease in the exit temperature of the working fluid (see Figure 11). On the other hand, when the geothermal source temperature decrease with respect to the design point, the working fluid flowrate is lowered and lesser quantity of working fluid than the design quantity passes through the fixed evaporator area. This causes an increase in the exit temperature of the working fluid from the evaporator and thus an increase in the level of working enthalpy parameter. After the peak point at 70 ^{o}C, the quantity of heat transferred from the geothermal is not enough to sustain the level of working fluid enthalpy parameter and thus the enthalpy parameter continues to fall as the geothermal source temperature continues to go down.

Figure 8: Effect of Variation in Geothermal Source Temperature on Working Fluid Flowrate & Enthalpy Parameter, $\varkappa$ at Turbine Inlet

Figure 9 shows the effect of variation in geothermal source temperature on the cooling water demand. The graph shows that as the geothermal source temperature increases, the cooling water demand continues to increase. This is because an increase in geothermal source temperature causes an increase in the working fluid flowrate. Hence, more cooling water is required to cool the increasing working fluid demand in the system. Also contained in the same graph is the variation in working fluid enthalpy parameter, $\varkappa$ at the pump inlet/condenser outlet as the geothermal source temperature changes. Using the plant design point as the reference, the working fluid enthalpy parameter at the condenser exit/pump inlet shows that the working fluid is always in the sub-cooled liquid state at temperatures above the geothermal design point; however, at temperature lower than the design temperature, the working fluid moves to the two phase region with small fraction of vapour. Although the vapour fraction is so small, this condition if not controlled may cause cavitation in the pump which will be detrimental to the operation of the system.

Figure 9: Effect of Variation in Geothermal Source Temperature on Cooling Water Mass Flowrate and Working Fluid Enthalpy Parameter at Condenser Outlet

Figure 10 shows the effect of variation in geothermal source temperature on the evaporator and condenser effectiveness. Increasing the geothermal source temperature higher than the design point increases the evaporator effectiveness and decreases the condenser effectiveness while decrease in the geothermal source temperature lower than the design point decreases the evaporator effectiveness and increases the condenser effectiveness.

Figure 10: Effect of Variation in Geothermal Source Temperature on Evaporator and Condenser Effectiveness

Figure 11 and 12 show the variation in the turbine inlet and outlet temperatures and pressures when the geothermal source temperature changes. As explained earlier, with reference to the design point, increasing the geothermal source temperature lowers the inlet turbine temperature. Also as shown in the graphs, both the outlet temperature and pressure of the turbine continues to increase as the geothermal source temperature increases.

Figure 11: Effect of Variation in Geothermal Source Temperature on Inlet and Outlet Turbine Temperature

Figure 12: Effect of Variation in Geothermal Source Temperature on Turbine Exit Pressure

5. Conclusion

It has been confirmed in this paper that the production of electricity from the low temperature geothermal sources using ORC system as claimed by Chena Power in the paper presented to the Alaska Energy Authority is a technologically feasible project. The IPSEpro PSE model of the Chena Geothermal ORC power plant developed in this paper is in close agreement with the plant design report presented by Chena Power. Although, the temperature of the geothermal source is likely to be fairly close to the design point, however, the effect of wide variation in the geothermal source temperature from the nominal design condition had been investigated in this report.

The analysis had shown that increase in the source temperature from the nominal design point will increase the plant output power up to a certain limit; however, this occurs at the detriment of the plant thermal efficiency which decreases.

Hence, it is recommended that ORC power plants should incorporate a great deal of automation so as to maintain the plant efficiency and design power output in order to avert the detrimental effect on plant performance associated with the variation in design operating conditions.

Acknowledgement

I wish to acknowledge by supervisors, Prof. Brian Agnew and Prof. Chris Underwood on the guidance and information they provided during the development of this article. I am also most grateful to them for proof reading the entire work.

References

[1] EIA, International Energy Statistics, in: U.S. Energy Information Administration Independent Statistics and Analysis, Department of Energy, USA, available at: www.eia.doe.gov, accessed 23 November, 2010.
[2] H.D.M. Hettiarachchi, M. Golubovic, W.M. Worek, Y. Ikegami, Optimum design criteria for an organic rankine cycle using low-temperature geothermal heat sources, Energy, 32 (2006) 1698-1706.
[3] M.H. Dickson, M. Fanelli, What is Geothermal Energy?, in: CNR-Istituto di Geoscience e Georisorse, Pisa, Italy, 2004, pp. 1-61.
[4] H. Leibowitz, I.K. Smith, N. Stosic, Cost effective small scale ORC systems for power recovery from low grade heat sources, in: Proceedings of 2006 ASME International Mechanical Engineering Congress and Exposition, Chicago, Illinois, USA, 2006, pp. 1-7.
[5] B.-T. Liu, K.-H. Chien, C.-C. Wang, Effect of Working Fluids on Organic Rankine Cycle for Waste Heat Recovery, Energy, 29 (2002) 1207- 1217.
[6] D. Wei, X. Lu, Z. Lu, J. Gu, Dynamic modeling and simulation of an Organic Rankine Cycle (ORC) system for waste heat recovery, Applied Thermal Engineering, 28 (2007) 1216-1224.
[7] G. Holdmann, 400kW Geothermal Power Plant at Chena Hot Springs, Alaska, in: Final Project Report Prepared for the Alaska Energy Authority, Chena Power Company, Alaska, 2007, pp. 1-37.
[8] G. Holdmann, The Chena Hot Springs 400kW Geothermal Power Plant: Experience Gained During the First Year of Operation, in: Chena Geothermal Power Plant Report, Chena Power Plant, Alaska, 2007, pp. 1-9.
[9] SimTech, IPSEpro PSE version 4.0, in: IPSEpro power generation and refrigeration library manual, SimTech Simulation Technology, available at: www.simtechnology.com, Austria, 2008.
[10] E.W. Lemmon, M.O. McLinden, M.L. Huber, REFPROP Reference Fluid Thermodynamic and Transport Properties, in: NIST Standard Reference Database 23, the US Secretary of Commerce, America, 2002.
[11] R.K. Shah, D.P. Sekulic, Heat Exchangers, in: W.M. Rohsenow, J.P. Hartnett, Y.I. Cho (eds.) Handbook of Heat Transfer, McGraw Hill, 1998, pp. 17.11 -17.169.
[12] J.E. Hesselgreaves, Compact Heat Exchangers: Selection, Design and Operation, Elsevier Science Ltd., Kidlington, Oxford, 2000.

Table(s)

Parameter	Nominal Value
Geothermal Source Temperature (^oC)	73.33
Geothermal Source Mass Flowrate (kg/s)	33.39
Cooling Water Source Temperature (^oC)	4.44
Cooling Water Source Mass Flowrate (kg/s)	101.68

Table 1

Table(s)

Molar Mass (kg/mol)	**Triple Point Temp (°C)**	**Normal B.P. (°C)**	**Critical Points**			**Range of Applicability**			
			Temp (°C)	Pressure (MPa)	Density (kg/m^3)	Min Temp (°C)	Max Temp (°C)	Max Pressure (MPa)	Max Density (kg/m^3)
102.03	-103.30	-26.07	101.06	4.06	511.90	-103.30	181.85	70.00	1591.70

Table 2

Table(s)

States	**Process**
1 – 2	The liquid working fluid is pumped to the pre-heater/evaporator/super-heater unit.
2 – 3	The working fluid is pre-heated in the pre-heater section at constant pressure using the heat from the geothermal source.
3 – 4	The working fluid is evaporated at constant temperature and pressure using the heat from the geothermal source.
4 – 5	The working fluid is superheated and turned completely into vapour using the geothermal heat source.
5 – 6	The super-heated vapour working fluid is expanded in the turbine to generate work.
6 – 7	The exit vapour working fluid from the turbine is de-superheated in the condenser.
7 – 1	The de-superheated working fluid is condensed completely to liquid to complete the cycle.

Table 3

Table(s)

Parameter	Real Power Plant Data	IPSEpro Simulation Result	
Geothermal Fluid Mass Flowrate (kg/s)	33.39	33.39**	0.00
Geothermal Fluid Temperature (°C)	73.33	73.33**	0.00
Cooling Water Mass Flowrate (kg/s)	101.68	101.68**	0.00
Cooling Water Source Temperature (°C)	4.44	4.44**	0.00
Working Fluid	R134a	R134a**	
Turbine Efficiency	0.80	0.80**	0.00
Turbine Inlet Pressure (bar)	16.00	16.95**	5.94
Turbine Outlet Pressure (bar)	4.39	4.39**	0.00
Gross Generator Power (kW)	250.00	250.00**	0.00
Pump Power (kW)	40.00	40.00**	0.00
Geothermal Exit Temperature (°C)	54.44	54.94*	0.92
Cooling Water Exit Temperature (°C)	10.00	9.91*	0.90
Working Fluid Mass Flowrate (kg/s)	12.17	11.99*	1.48
Net Plant Power (kW)	210.00	210.00*	0.00
Thermal Efficiency	0.08	0.08*	0.00
Evaporator Heat Transfer Rate (kW_{th})	2580.00	2570.38*	0.37
Condenser Heat Transfer Rate (kW_{th})	2360.00	2327.10*	1.39
Evaporator UA value (kW)	------	119.28*	-----
Condenser UA Value (kW)	------	336.04*	-----

Evaporator (NTU)	------	0.85*	-----
Condenser (NTU)	------	0.79*	-----
Evaporator Effectiveness (ε)	------	0.30*	-----
Condenser Effectiveness (ε)	------	0.45*	----
Working Fluid Enthalpy Parameter at Turbine Inlet	------	1.04*	----
Working Fluid Enthalpy Parameter at Turbine Exit	------	1.02**	----

****set variables, *calculated variables from the IPSEpro simulation**

Table 4

Table(s)

Parameter	**Fixed Value**
UA value of the Evaporator	119.28 kW/K
UA value of the Condenser	336.04 kW/K
Geothermal Exit Temperature	54.94 ^{o}C
Cooling Water Exit Temperature	9.91 ^{o}C
Turbine Inlet Pressure	16.95 bar
Temperature at Evaporator Inlet	12.85 ^{o}C

Table 5

Figure(s)

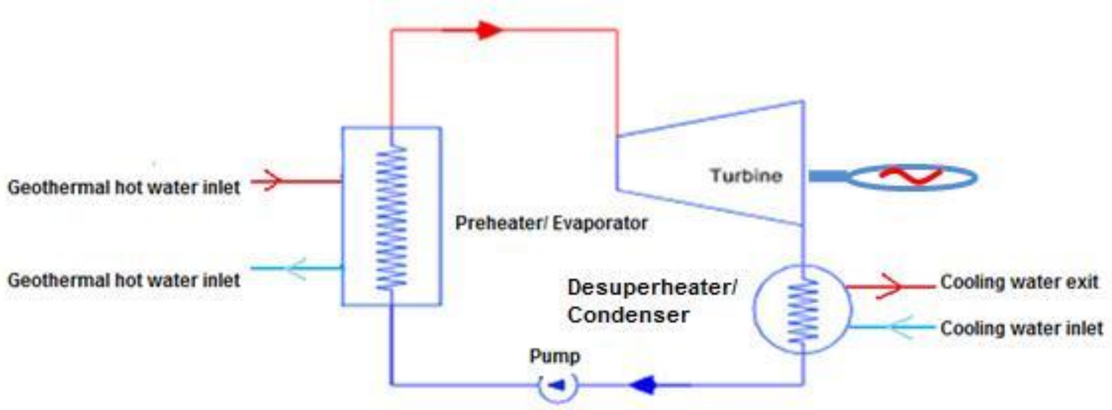

Figure 1

Figure(s)

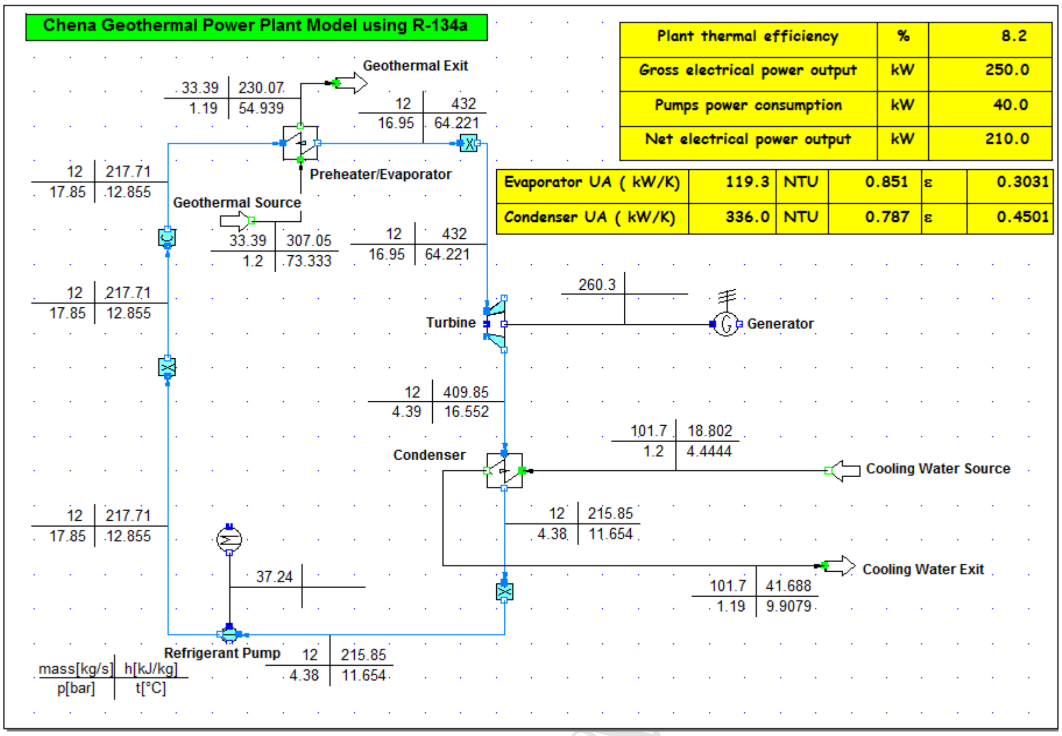

Figure 2

Figure(s)

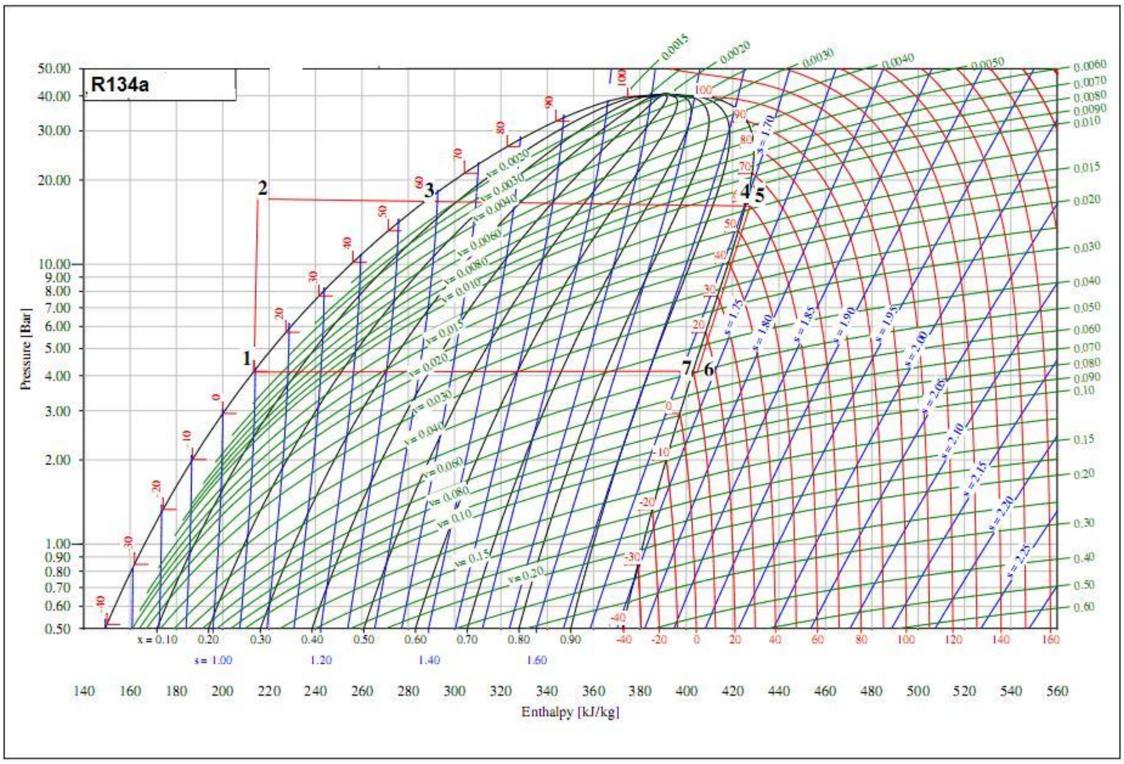

Figure 3

Figure(s)

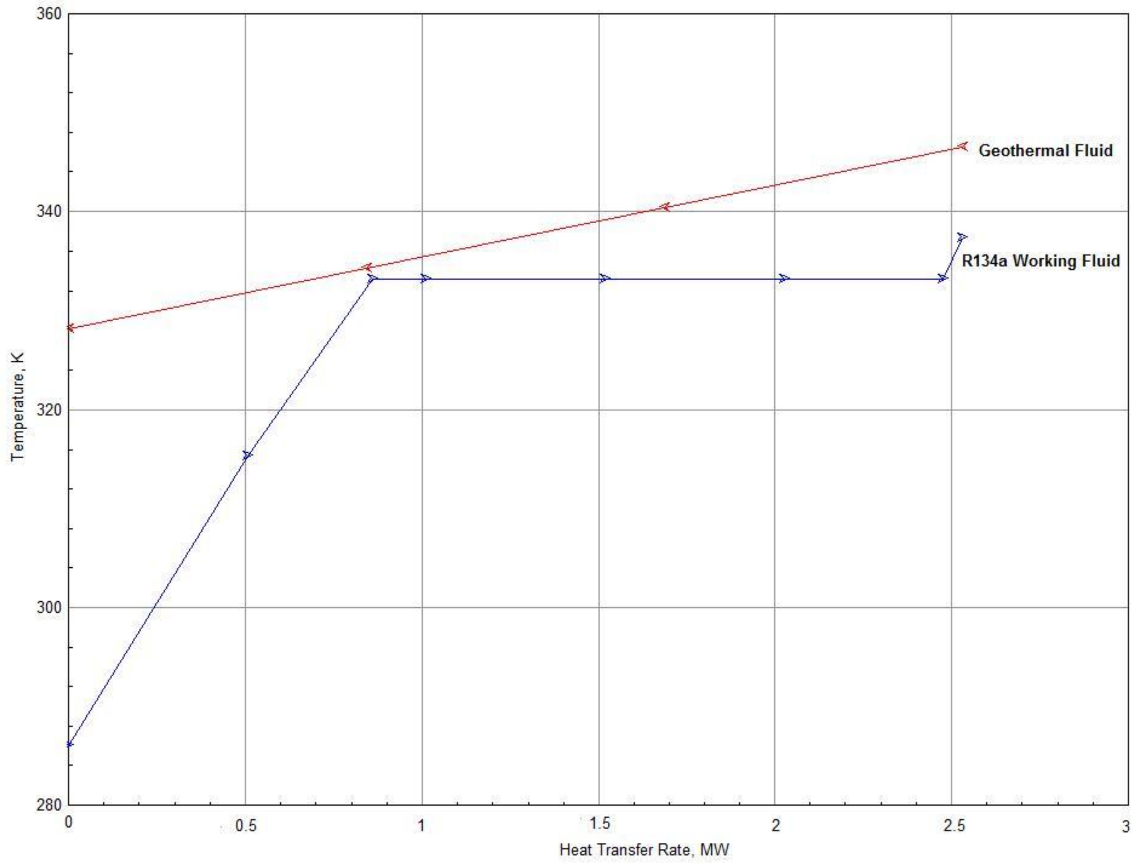

Figure 4

Figure(s)

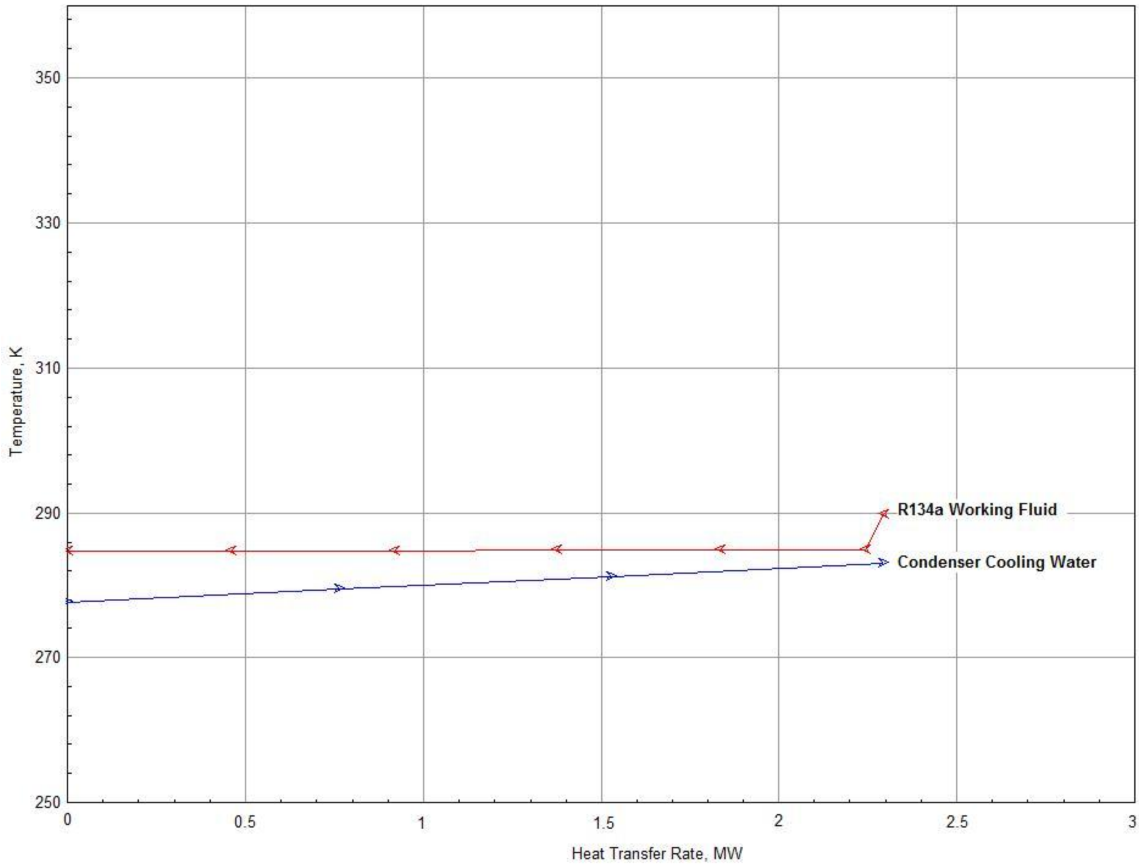

Figure 5

Figure(s)

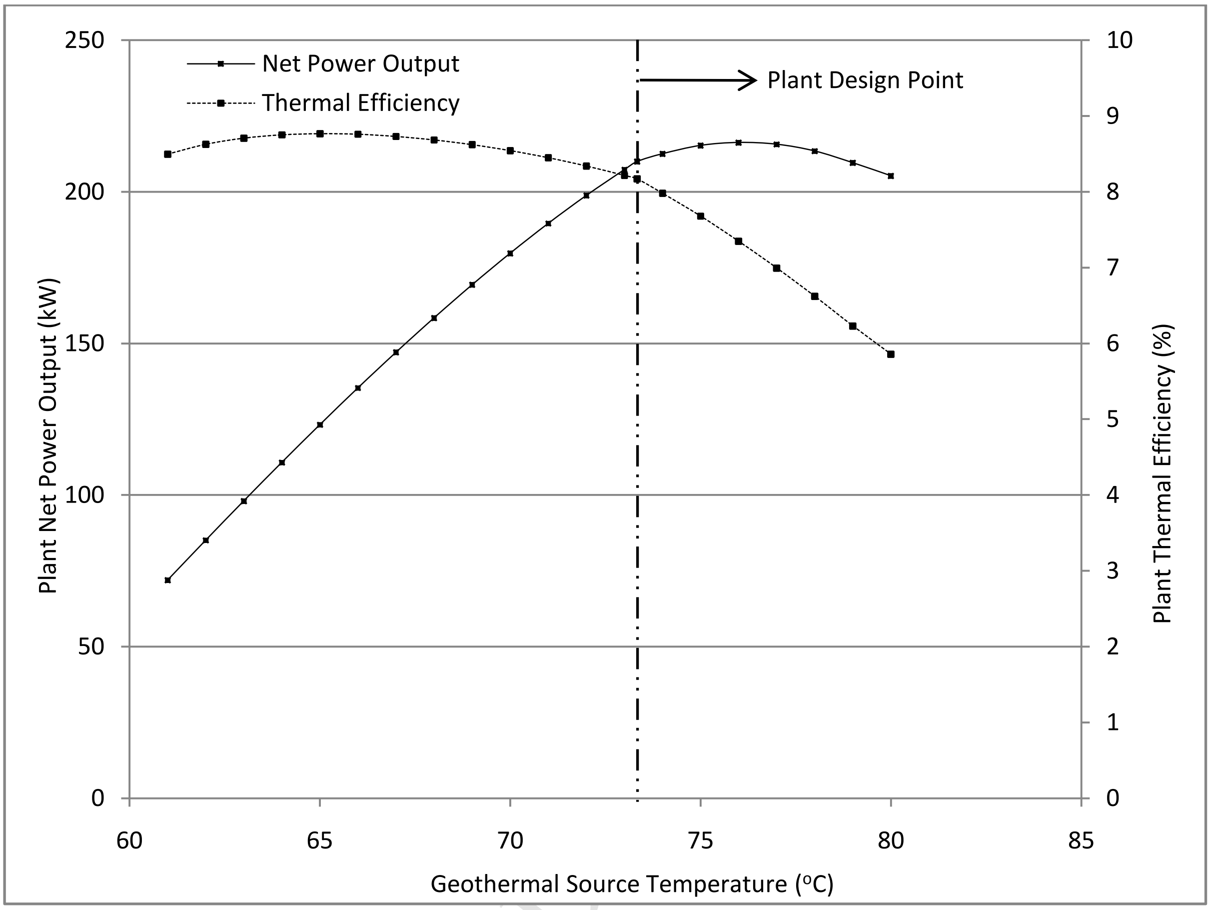

Figure 6

Figure(s)

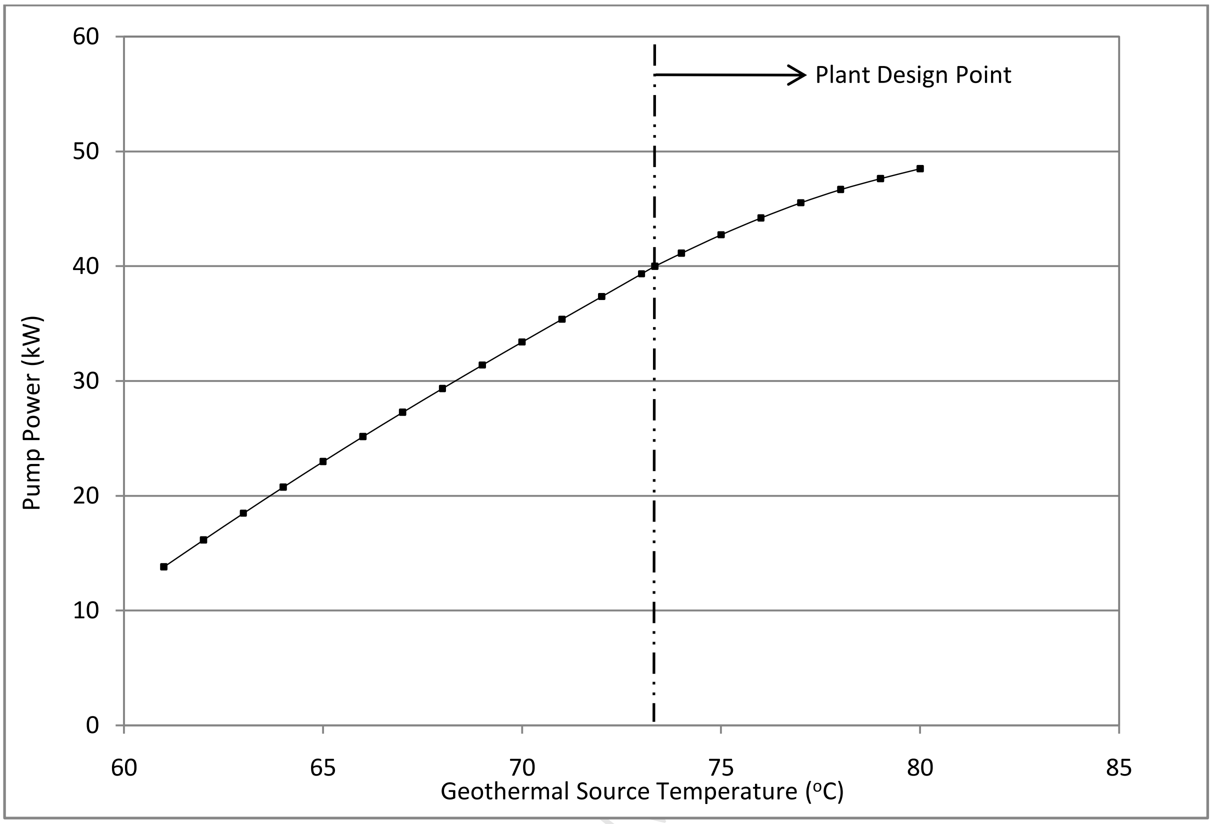

Figure 7

Figure(s)

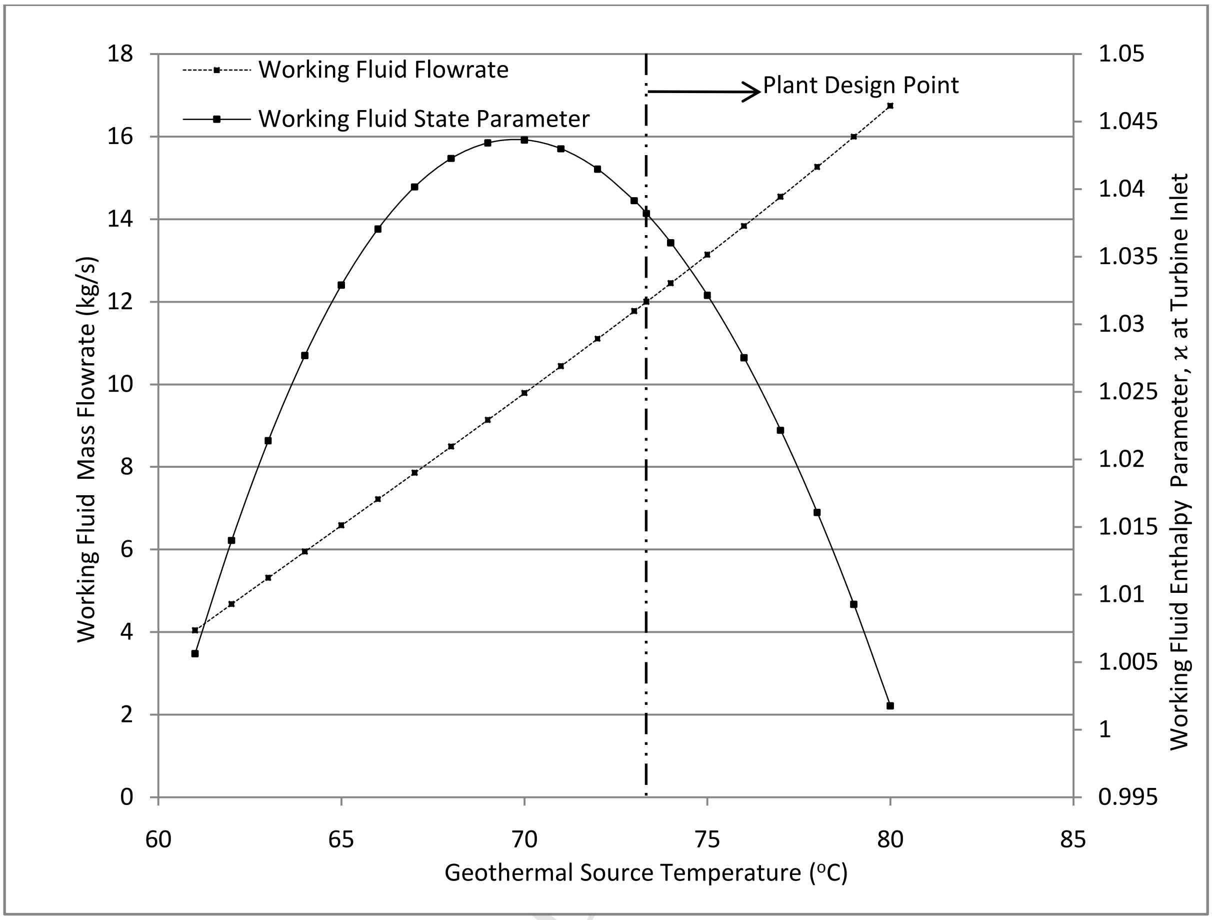

Figure 8

Figure(s)

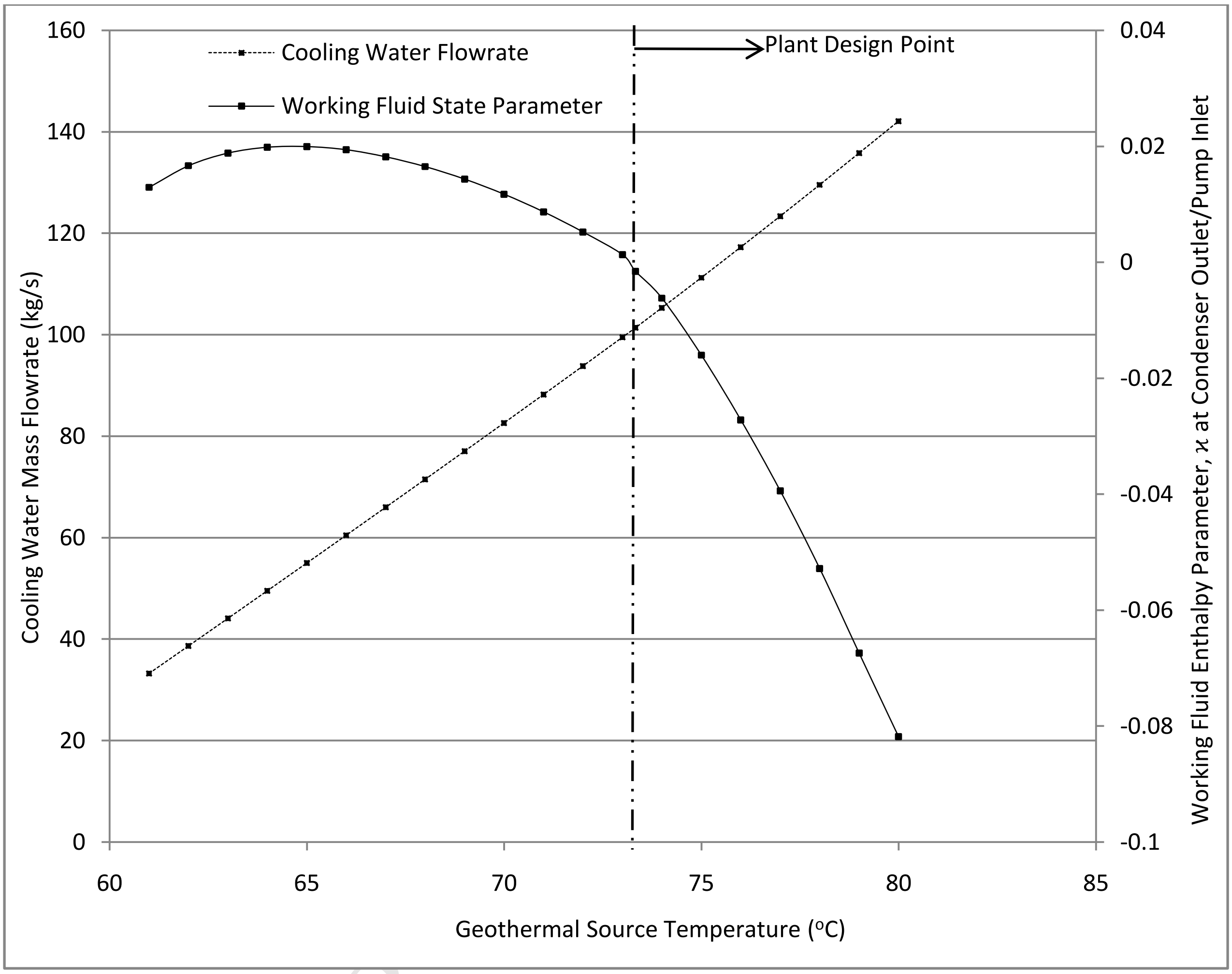

Figure 9

Figure(s)

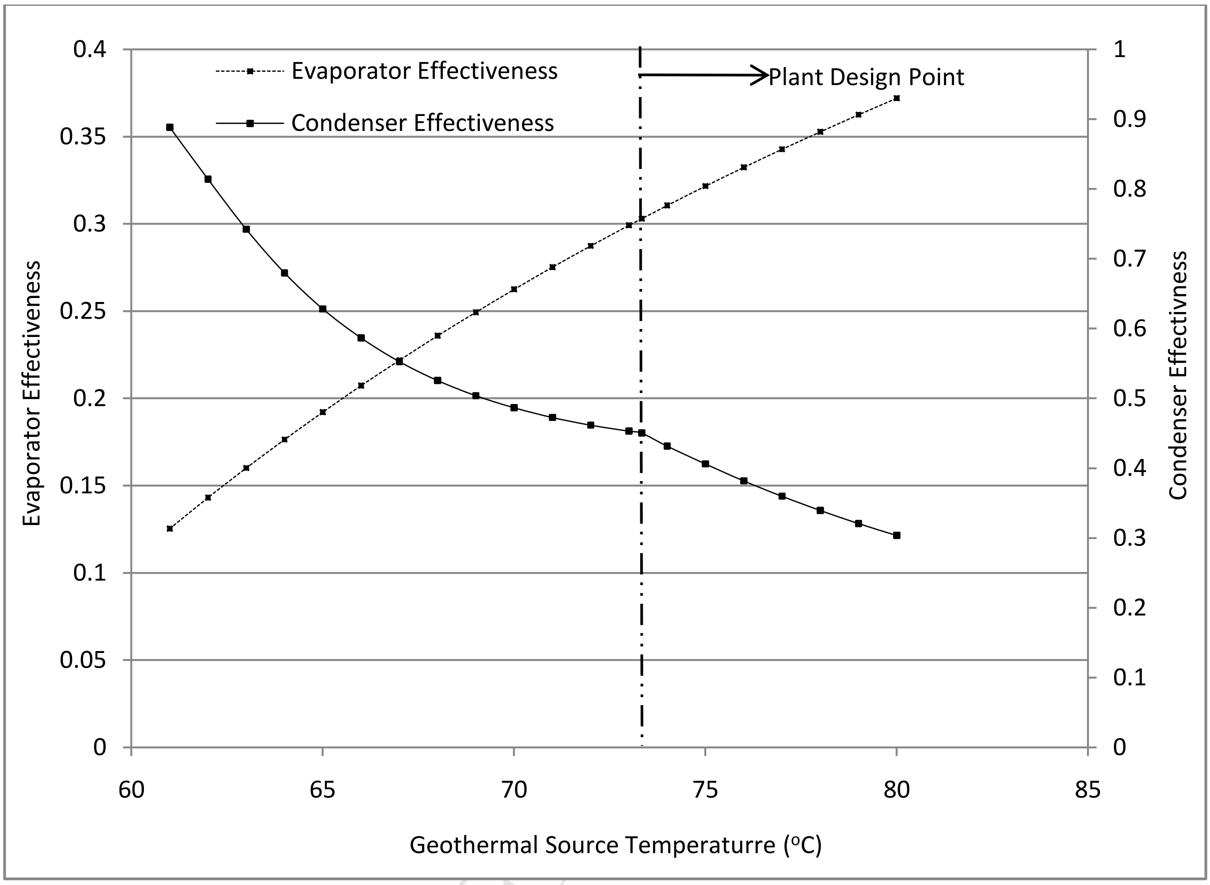

Figure 10

Figure(s)

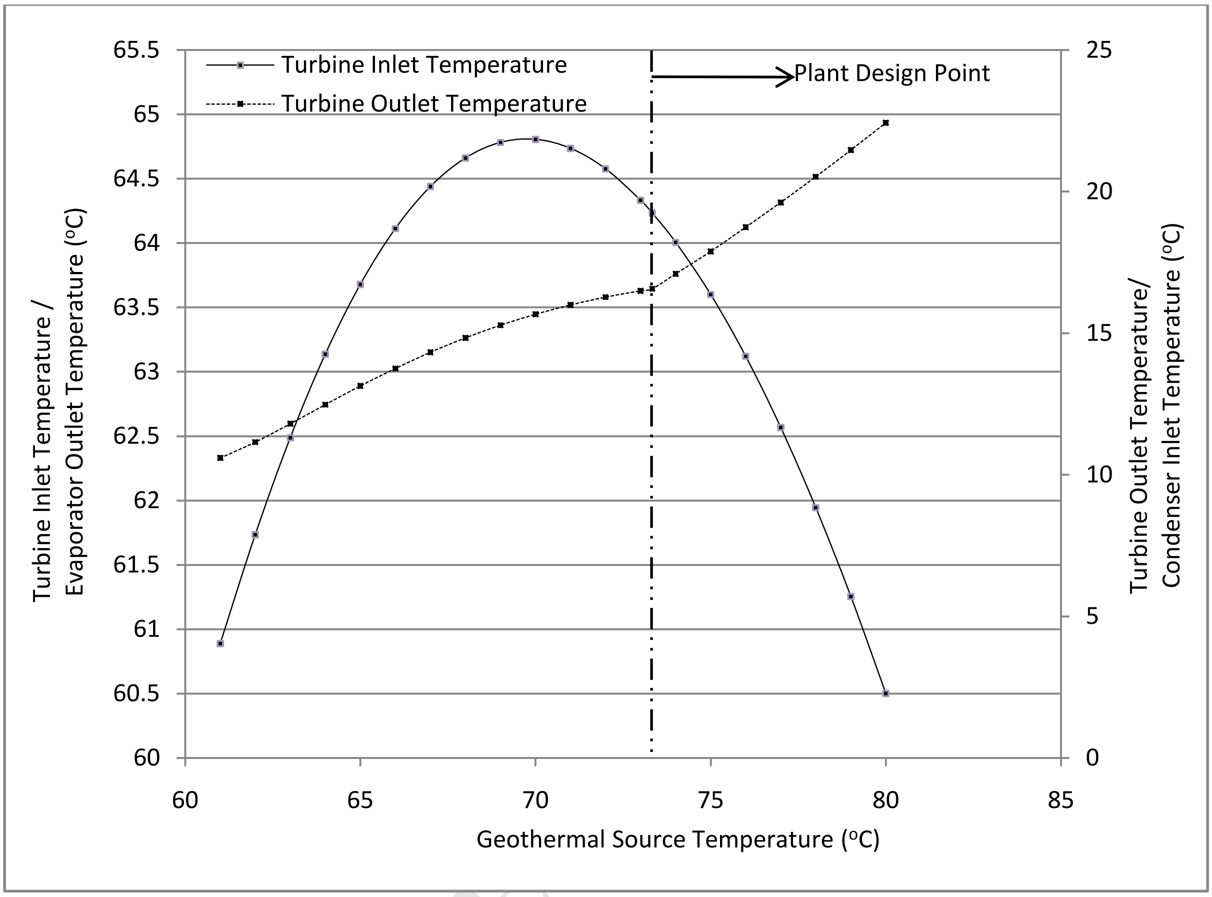

Figure 11

Figure(s)

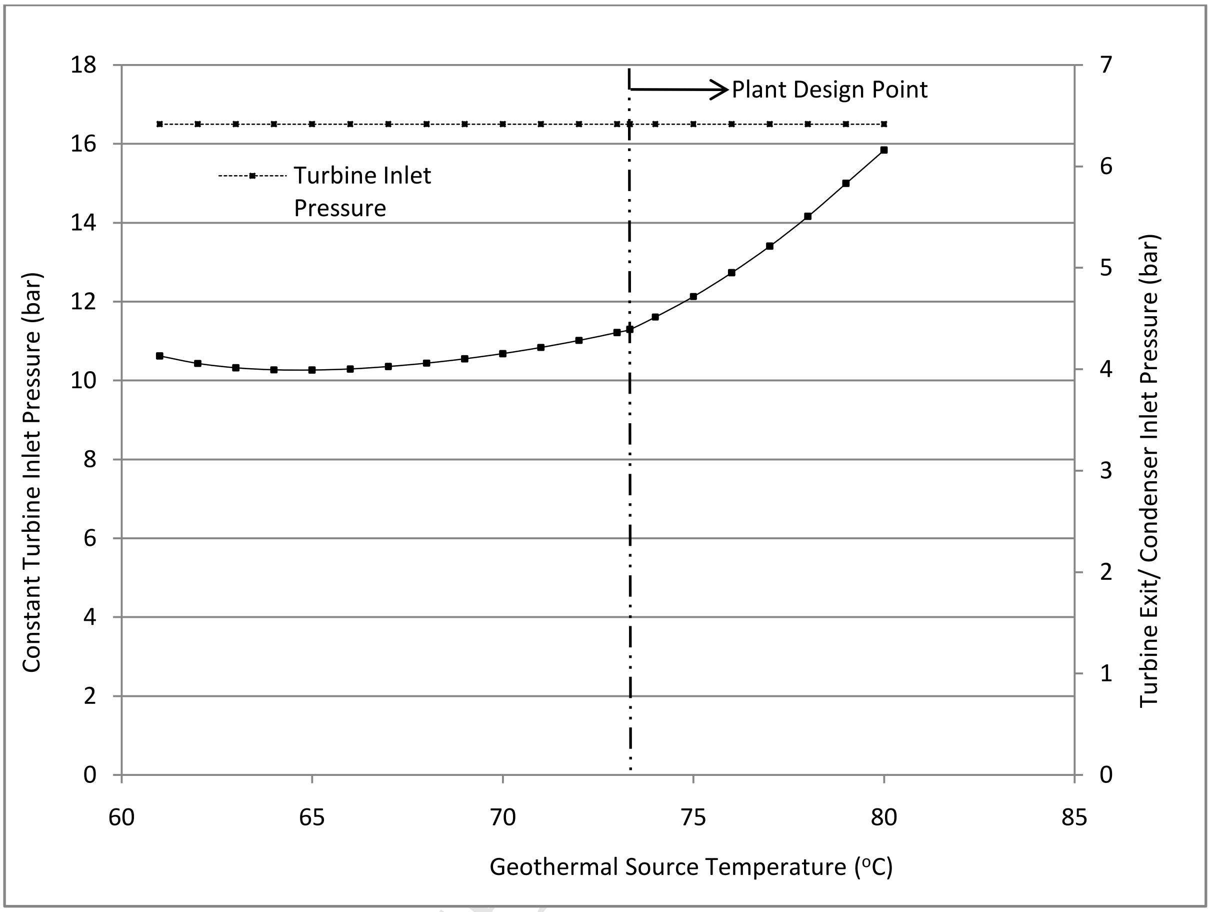

Figure 12